Remote Sensing and Geophysical Exploration for Uranium-Mineralized Breccia Pipes in Northwestern Arizona, USA

Kwarteng, Y. A.
Sultan Qaboos University, Remote Sensing and GIS Center
Box 33, Al-Khod PC 123, Sultanate of Oman
Email: kwarteng@squ.edu.om

Abstract

Exploration for uranium-mineralized breccia pipes in northwestern Arizona, USA, has generated interests for several years. These deposits contain high-grade uranium ore and by-products such as Ag, Au, Cu, Pb, Zn, and V. The breccia pipes were formed from the collapse of the overlying sedimentary strata into karst caverns developed in the Mississippian Redwall Limestone. The breccia pipes are known to occur in clusters and are commonly observed along the cliffs of the Grand Canyon and other near-by canyons. On undissected areas of northwestern Arizona part of the Colorado Plateau, the pipes appear as circular features with concentrically inward dipping beds. For most of the known deposits, hydrothermal alteration associated with the uranium-mineralization is concealed under veneer of soil. In this study, digitally enhanced Landsat Thematic Mapper (TM) images were used to identify more than 80% of previously known orebodies as well as additional anomalies. In addition, digital image processing and integration of datasets were used to develop exploration models from airborne electromagnetics (EM) , mangetics and very-low-frequency electromagnetics (VLF-EM) data collected over an area in northwestern Arizona. One of the best models incorporated apparent resistivity and total magnetic; the results of this model outlined 13 anomalous areas for further investigation.

Introduction

Mining for metals in the Grand Canyon area in United States of America commenced in the 19th Century and since then uranium, copper, zinc, gold, and silver have been mined from many deposits (Foord et al., 1978; Keith et al., 1983). Some of the deposits were later recognized as breccia pipes. The main commodity exploited from the breccia pipes has shifted from copper to uranium since the 1950s. Fig. 1 shows the location of past mines, current mines, possible orebodies, and identified breccia pipe mineral occurrences in northwestern Arizona. More than

20 orebodies have been discovered since the late 1970s. Old mines (developed before 1980) from which uranium was produced are the Orphan, old Hack Canyon, Riverview, Ridenour, Parashant, and Chapel (Pierce et al., 1970; Keith et al., 1983). The first major uranium breccia pipe deposit was the Orphan mine, which produced over 500,000 tons of ore with an average grade of 0.42% U_3O_8 between 1956 and 1969 (Pierce et al., 1970; Chenoweth, 1986). Between 1980 and 1986, more than 10 million lbs. of uranium with an average grade of 0.65% U_3O_8 were mined from breccia pipes in northwestern Arizona (Mathisen and Energy Fuels Corporation Staff, 1987).

The formation of breccia pipes is directly related to the karst topography developed in the Mississippian Redwall Limestone. The collapse and additional movement accompanying the formation of breccia pipes have in some cases affected more than 1,000 m of strata transgressing formation boundaries between the Redwall Limestone and the Triassic Chinle Formation. The intrapipe fragments, which are rounded to angular, range from a few to tens of meters. Breccia pipes have not been observed in formations older than the Redwall Limestone or in those younger than the Chinle Formation. In theory, all areas on the Colorado Plateau underlain by the Redwall Limestone are permissive for the occurrence of mineralized breccia pipe deposits. Mineralization of the breccia pipes occurred within the interval 200-220 million years ago as determined from U-Pb isotopic analysis (Ludwig et al., 1986). The mineralizing fluids are believed either to have moved up or down the pipes before they were reduced (Kwarteng, 1988).
The morphology of a breccia pipe consists of two main interrelated parts: the throat and the collapse cone (Fig. 2). The throat consists of a volume of brecciated rocks that have been downdropped from the original stratigraphic level. The brecciated rocks are separated from the country rock by a fracture zone which has been referred to as the ring fracture (Wenrich, 1985). The throat of a breccia pipe is cylindrical with a nearly vertical axis (Fig. 2). The diameter commonly varies from 30 m to 100 m. Along the vertical axis within a particular pipe, there can be a flexure in the axis and a change in the diameter ranging from 30 m to 2.4 km, but commonly less than 250 m. Alteration associated with the breccia pipes consist of reduction, which resulted from ore deposition, and oxidation, which presumably occurred after the ore was formed.
The surface expressions characteristics of mineralized breccia pipes may include all or some of the following: (1) concentrically inward dipping beds, (2) circular patches of brecciated rocks,

(3) bleached or limonite stained rock, (4) circular concave topography, (5) circular vegetation changes, and (6) gamma radiation in excess of 2.5 times the background (Wenrich, 1985). On the undissected parts of the Colorado Plateau in northwestern Arizona, the surface expression of a mineralized breccia pipe is often subtle and recognition is becoming more and more challenging to geologists, especially as the majority of the easily identifiable pipes in the region have been discovered. Fig. 3 shows an exposed breccia pipe on the north wall of the Little Colorado River gorge.

Exploration techniques for mineralized breccia pipes include ground and airborne geophysics; soil, water, and rock geochemistry; helium soil-gas; and Bacillus cereus (Wenrich, 1986). The results have often been mixed, and the importance placed on an individual technique varies from one exploration group to another. The most common reconnaissance technique entails mapping circular features on color aerial photographs at a scale of 1:24,000 or larger. The anomalies are subsequently evaluated by more intensive investigation including field mapping, shallow drilling to determine any dipping structure, geophysical and geochemical surveys. A detailed knowledge of the stratigraphy of the area is essential in determining downdropped units, especially within the same formation.

In this study, Landsat Thematic Mapper imagery (TM) and color infrared photograph were digitally enhanced and used map circular features with the potential for the occurrence of mineralized breccia pipes. In addition, digital image processing and integration of datasets were used to develop exploration models from airborne electromagnetics (EM), mangetics and very-low-frequency electromagnetics (VLF-EM) data collected over an area in northwestern Arizona.

Methodology

The digital enhancement techniques that were applied to the Landsat TM imagery with a spatial resolution of 30 m/pixel and color infrared photograph (National High Altitude Aerial Photography (NHAP)) included: (1) contrast stretching, (2) band ratioing, (3) principal component (PC) analysis (4) vegetation suppression and (5) spatial filtering. The objectives were to map circular and hydrothermally altered breccia pipes surfaces from the surroundings. In some of the areas where vegetation cover was more than 40%, vegetation was suppressed in order to emphasize the soil and lithology (Kwarteng, 1988). The NHAP image of part of the study area was digitized with blue, green and red filters to obtain three images. The images were enhanced

to improve the visual appearance of structural features which might suggest potential breccia pipes occurrences.

Digital processing techniques applied to the airborne geophysical data included: (1) conversion of the data into gridded raster images, (2) spatial filtering for noise removal, (3) integration and analysis of datasets, and (4) modeling using various combinations of the geophysical variables (Kwarteng, 1988; Kwarteng and Chavez, 1990). To generate a black-and-white image of the individual geophysical variables, the data were converted into 8-bit integer digital numbers (DNs) that correspond to a range of 0-255, representing 256 gray-level DNs that may be shown on an image display device. Minimum and maximum DN values for contrast stretching were selected on the basis of the distribution of the frequency histogram of each variable. Contrast stretching transforms the digital values that are present in the image over the entire 0 to 255 dynamic range available (Kwarteng, 1988; Kwarteng and Chavez, 1990).

Results and Discussion

The most useful Landsat TM images for mapping circular features were: (1) color composites generated from one of the visible TM bands, band 4 and bands 5 or 7, (2) high-pass filter (HPF) image of TM band 2 or 7 and (3) color composite image of the TM visible bands (Kwarteng, 1988). For areas with more than 30% vegetation cover, it was necessary to digitally mask the image to remove the major effects of vegetation in order to better observe features relating to the soil and rock. Fig. 4 is an enhanced Landsat TM bands 5, 4 and 3 color composite image of the Hack area showing the location of known know orebodies and potential/suspected targets orebodies. Fig. 5 shows an HPF (kernel size 51 by 51) image of Landsat TM band 7 of the Hack area. Digitally enhanced TM images printed at the scale of 1:100,000 resulted in the recognition of more than 80% of previously known orebodies as well as additional anomalies identified in the study areas. Twenty-six and 30 potential targets in the Hack and Hualapai study areas, respectively, were selected as potential targets for the occurrence of breccia pipes. In areas with more than 30% vegetation cover, low altitude color aerial photographs printed at 1:58,000 appeared to be the most useful for mapping circular and linear features (Fig. 6).

The general relationships between the geophysical variables and their ability to detect metallic deposits were used as guides in further analysis and image interpretation. The relationship between breccia pipes in northwestern Arizona and the geophysical parameters indicated the

following: (1) breccia pipes are characterized by highly conductive central zones surrounded by highly resistive hosts (Flanagan et al., 1986); (2) breccia pipes found in the survey area tend to exhibit anomalously high magnetic susceptibility, compared to the surrounding country rocks, because of the presence of relatively large quantities of magnetic minerals in the preserved downdropped Moenkopi blocks; (3) the overburden depths over breccia pipes on the North Rim of the Grand Canyon area, determined from drill hole data, are thicker than over the surrounding areas because of the downdropped Moenkopi rocks; and (4) the VLF-EM values over mineralized breccia pipes have been found to be inconsistent (i.e., low, average, and high). In the model that incorporated VLF-EM data, it was assumed that the values were high over breccia pipes because of the downdropped Moenkopi rocks.

The upper and/or lower 20% DNs, depending on the variable, were selected as the cutoff limits for separating areas of interest (Kwarteng and Chavez, 1990). The upper and lower 20% cutoffs were selected empirically from inspection of the frequency histograms of the individual images. The 20% value was a conservative choice and included what was considered either high or low for the given image. The lower 20% DN values of the apparent resistivity, and the upper 20% of the total-field magnetics, derived overburden thickness, and VLF-EM, respectively, were selected as the threshold cutoff values and used as input into the modeling algorithm. The threshold DN values were: (1) resistivity ≤83 (≤160 ohm-m), (2) magnetics ≥132 (≥51 809 nT), (3) overburden thickness ≥128 (≥40 m), and (4) VLF-EM ratios ≥118 (≥4) (Kwarteng, 1988). Boolean operations were used to identify pixels whose DN values in each geophysical variable were within the DN ranges selected. This technique assigns output DN values to a pixel based on the various cutoff input DN (i.e., wide or inside the selected ranges).

Four models were created using different combinations of the geophysical data (Fig. 7). The models have been color-added to show where the various combinations occurred. The first model (Fig. 7a) combined resistivity, magnetics, VLF-EM, and overburden thickness. Model 2 (Fig. 7b) consisted of resistivity, magnetics, and overburden thickness. Model 3 (Fig. 7c) combined resistivity, magnetics, and VLF-EM. Model 4 (Fig. 7d) was created by using only the resistivity and magnetic images because of the redundancy between resistivity and overburden thickness. The red color in Fig. 7 represents locations where all the input datasets were anomalous as defined by the previously described thresholds. These areas, referred to as anomalies, have the highest potential for the occurrence of breccia pipes. In model 1 the anomalies represent 5.13%

of the total area, 11.25% in model 2, 5.68% in model 3 and 12.04% in model 4. Comparison of models 1 and 3 (Fig. 7a and 7c) shows that they have 10 and 12 anomalies, respectively, regardless of the size of the anomalies. The number of anomalies in models 1 and 3 are present in models 2 and 4 as well. Models 2 and 4 have the same number of anomalies, but in the latter some of the areas of interest are larger or the shapes (circulatory) are better than the other because (1) it excluded VLF-EM measurements that are found to be inconsistent over known mineralized breccia pipes and can confuse the results, except for structural interpretation, and (2) the redundancy between resistivity and overburden thickness was avoided so that the same results were generated with one less variable, which made the processing easier and faster. Model 4 with 13 anomalies (Fig. 7d) which account for approximately 12% (1.9 km^2) of pixels in the survey area is the most recommended model.

The validity and utility of the results obtained with any model are dependent on the reliability of the input datasets and the logic used in selecting specifications. The ability to locate previously known deposits can be used to test the reliability of the data sets. The capability to predict favorable areas for future exploration is also important. Field checking confirmed that anomalies F and H in Fig. 7d correspond to EZ-2 and What orebodies. Anomaly G represents the EZ-4 pipe, where minerals associated with mineralized pipes have been found. However, one other known orebody, EZ-1, located less than 30 m east of anomaly I was not conclusively identified. A study of the survey flight lines and the anomalies in Fig. 7d indicates that anomalies F, H, and G are crossed by 4 or 5 flight lines, whereas the area representing the location of EZ=1 is crossed at its edge by only one flight line. This may account for the absence of EZ-1 in Fig. 7d. Most of the remaining anomalies correspond to target areas identified independently by the exploration company involved in the project. From the morphology of breccia pipes and the shape of known orebodies in Fig. 7d, anomalies L, M, and E have a higher potential than do A, B, C, D, J, and K.

Conclusions

Exploration for uranium-mineralized breccia pipes in northwestern Arizona, USA, has been quite active even during times of low price for the metal because of the high-grade and potential by-products such as copper, zinc, gold, and silver. The formation of breccia pipes is directly related

to the karst topography developed in the Mississippian Redwall Limestone. On undissected areas of northwestern Arizona part of the Colorado Plateau, the pipes appear as circular features with concentrically inward dipping beds.

In this study, digitally enhanced Landsat TM and color infrared images were used to map circular and other feature with potential for the occurrence of mineralized breccia pipes. Twenty-six and 30 potential targets in the Hack and Hualapai study areas, respectively, were selected as potential targets for the occurrence of breccia pipes. In areas with more than 30% vegetation cover, low altitude color aerial photographs printed at 1:58,000 appeared to be the most useful for mapping circular and linear features. Digital image processing and integration of datasets were used to develop exploration models from airborne electromagnetics, mangetics and VLF-EM data collected over an area in northwestern Arizona. One of the best models incorporated apparent resistivity and total magnetic; the results of this model outlined 13 anomalous areas, representing approximately 12% (1.9 km²) of the study for further investigation. As is generally the case, the output products of most models used in exploration only suggest areas of potential interest for further investigation. The use of digitally integrated geophysical data and processing technique considerably narrowed the area of interest. The next step is to go to these areas and use conventional physical exploration techniques. In this particular case, field geologic and structural mapping is essential for further appraisal of the significance of each anomaly for the potential occurrence of mineralized breccia pipes.

References

Chenoweth, W.L. (1986), The Orphan lode mine, Grand Canyon, Arizona – A case history of a mineralized, collapse-breccia pipe, U.S. Geological Survey. Open-File Report 86-510.

Flanagan, V.J., Mohr, P., Tippens, C., and Senterfit, M. (1986), Electrical character of collapsed breccia pipes on the Coconino Plateau, northern Arizona, U.S. Geological Survey Open-File Report 86-521.

Foord, E.E., McKee, E.D., and Bowles, C.G. (1978), Status of mineral resource information for the Shivwits Plateau, Parashant, Andrus, and Whitmore Canyons, and Kanab Canyon areas, Grand Canyon, Arizona, U.S. Geological. Survey Administrative Report for the Natl. Park Service.

Keith, S.B., Gest, D.E., DeWitt, E., Toll, N.W., and Everson, B.A. (1983), Metallic mineral districts and production in Arizona, Arizona Bureau of Geology and Mineral Technical. Bulletin no. 194.

Krewedl, D.A., and Carisey, J.C. (1986), "Uranium mineralized breccia pipes in northern Arizona", *Arizona Geological. Society Digest*, Vol. 16, pp. 179-186.

Kwarteng, A.M.Y. (1988), Remote sensing applied to the exploration for uranium-mineralized breccia pipes in northwestern Arizona, Ph.D. dissertation, University of Texas at El Paso, USA.

Kwarteng, A.Y., and P.S. Chavez, Jr. (1990), "Digital image processing of airborne geophysical data for uranium-mineralized breccia pipes exploration in northwestern Arizona", *Geophysics*, Vol. 55, pp. 965-976.

Ludwig, K.R., Rasmussen, J.D., and Simmons, K.R. (1986), Age of uranium ores in collapse-breccia pipes in the Grand Canyon area, Northern Arizona, Bulletin. American Rocky Mountain Section Annual. Meeting, 39, Abstracts with Program, pp. 392.

Mathisen, Jr. I.W. and Energy Fuels Corporation Staff (1987), Arizona Strip breccia pipe exploration program: development, and production, Bulletin American Association of Petroleum Geology 71/5, pp. 590.

Pierce, H.W., Keith, S.B., and Wilt, J.C. (1970), Coal, oil, natural gas, helium, and uranium in Arizona, Arizona Bureau Mines Bulletin 182.

Wenrich, K.J. (1985), "Mineralization of breccia pipes in northern Arizona", Economic Geology Vol. 80, pp. 1722-1735.

Wenrich, K.J. (1986), "Geochemical exploration for mineralized breccia pipes in northern Arizona, USA", Applied Geochemistry Vol. 1, pp. 469-485.

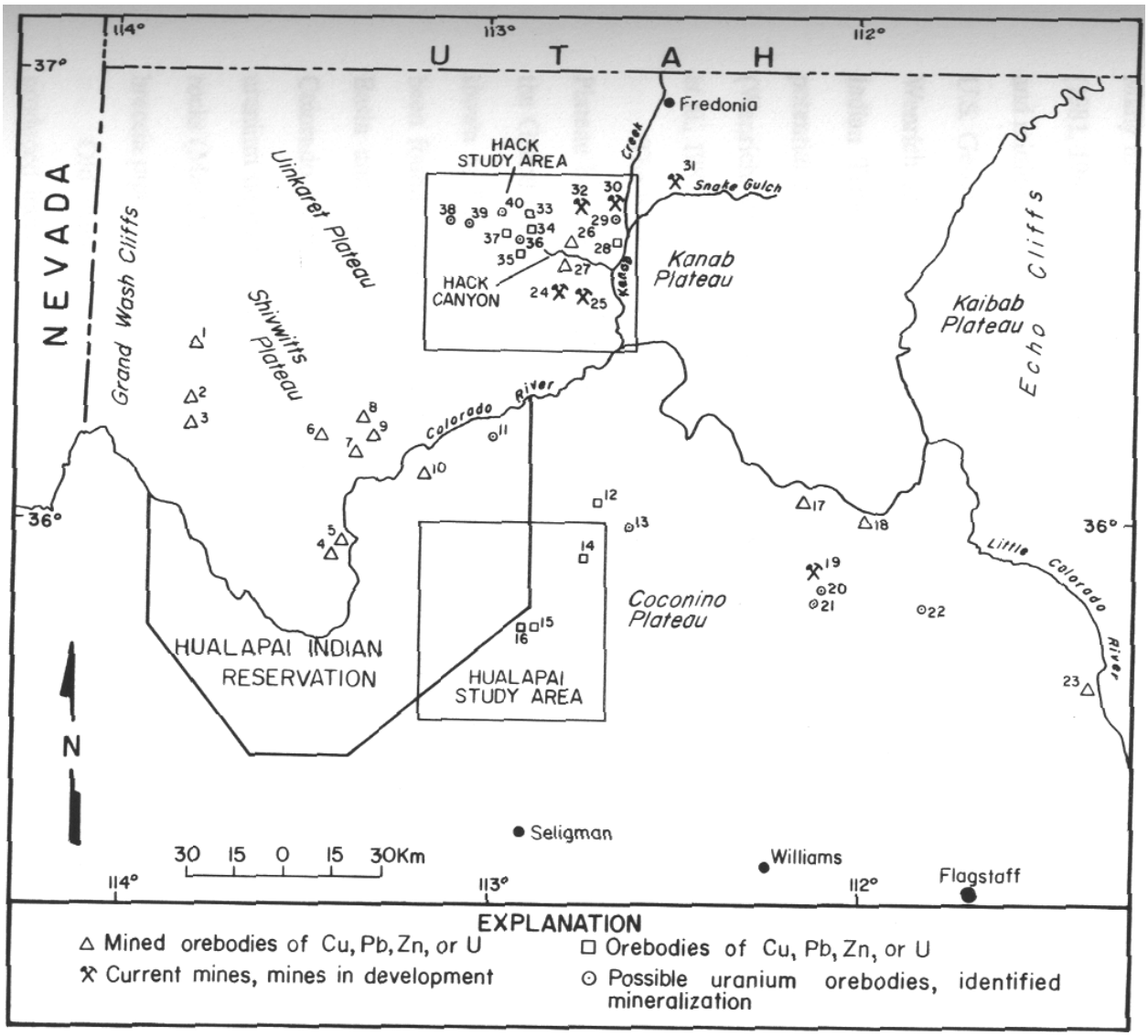
114°
113°
112°
37°
36°
U T A H
NEVADA
Fredonia
HACK STUDY AREA
HACK CANYON
Snake Gulch
Kanab Creek
Kanab Plateau
Kaibab Plateau
Echo Cliffs
Grand Wash Cliffs
Uinkaret Plateau
Shivwitts Plateau
Colorado River
Little Colorado River
Coconino Plateau
HUALAPAI INDIAN RESERVATION
HUALAPAI STUDY AREA
N
30 15 0 15 30Km
Seligman
Williams
Flagstaff
EXPLANATION
△ Mined orebodies of Cu, Pb, Zn, or U
□ Orebodies of Cu, Pb, Zn, or U
⚒ Current mines, mines in development
⊙ Possible uranium orebodies, identified mineralization

Fig. 1.

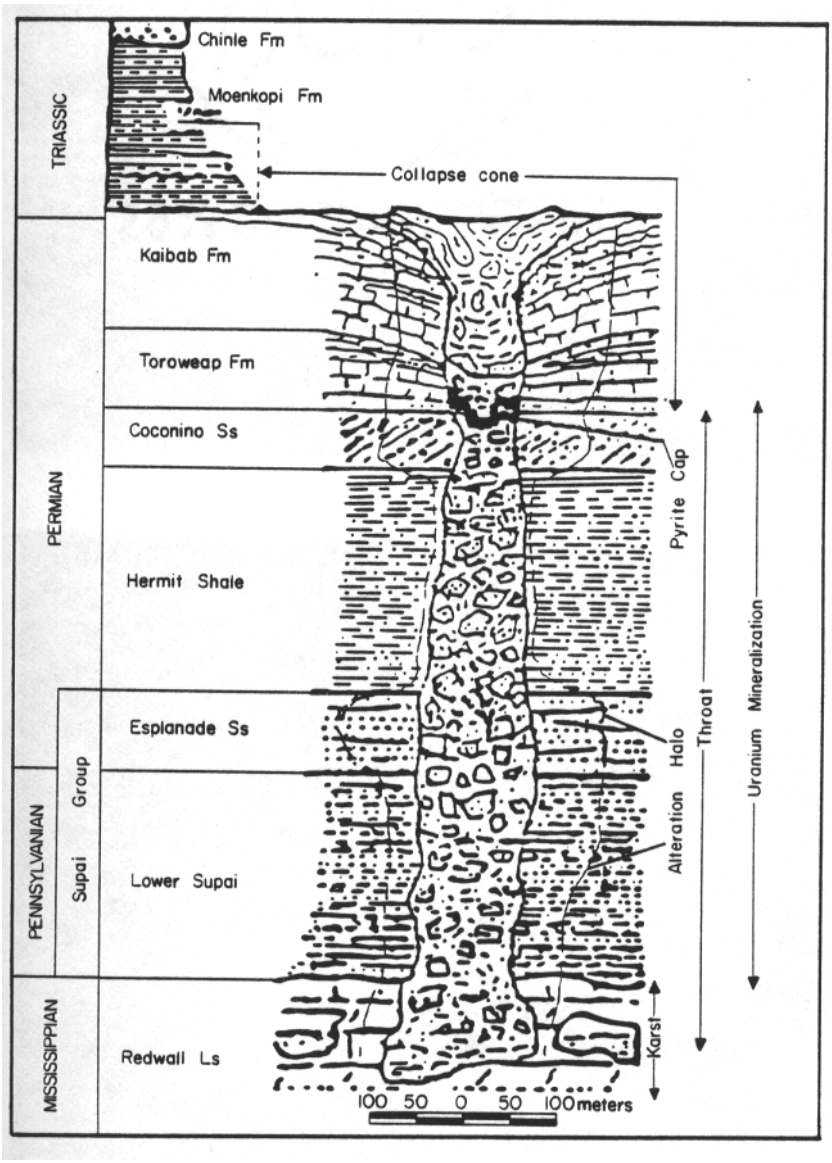
TRIASSIC
PERMIAN
PENNSYLVANIAN
MISSISSIPPIAN
Supai Group
Chinle Fm
Moenkopi Fm
Collapse cone
Kaibab Fm
Toroweap Fm
Coconino Ss
Hermit Shale
Esplanade Ss
Lower Supai
Redwall Ls
Pyrite Cap
Halo
Alteration
Throat
Karst
Uranium Mineralization
100 50 0 50 100 meters

Fig. 2.

A

B

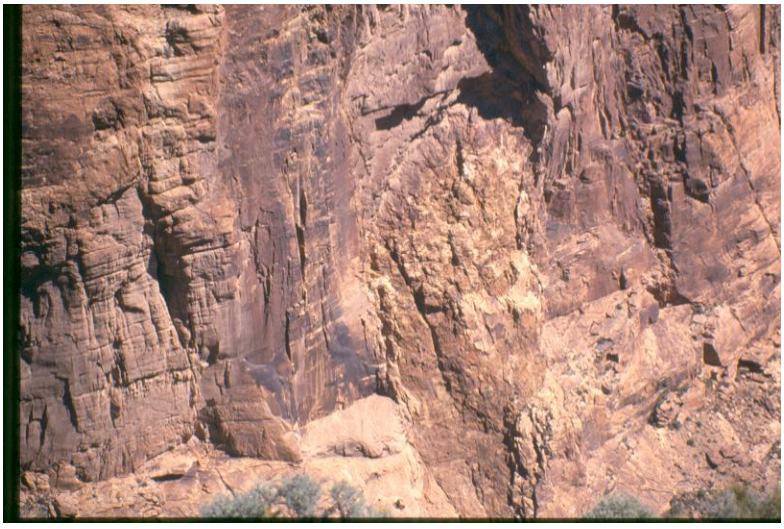

Fig. 3.

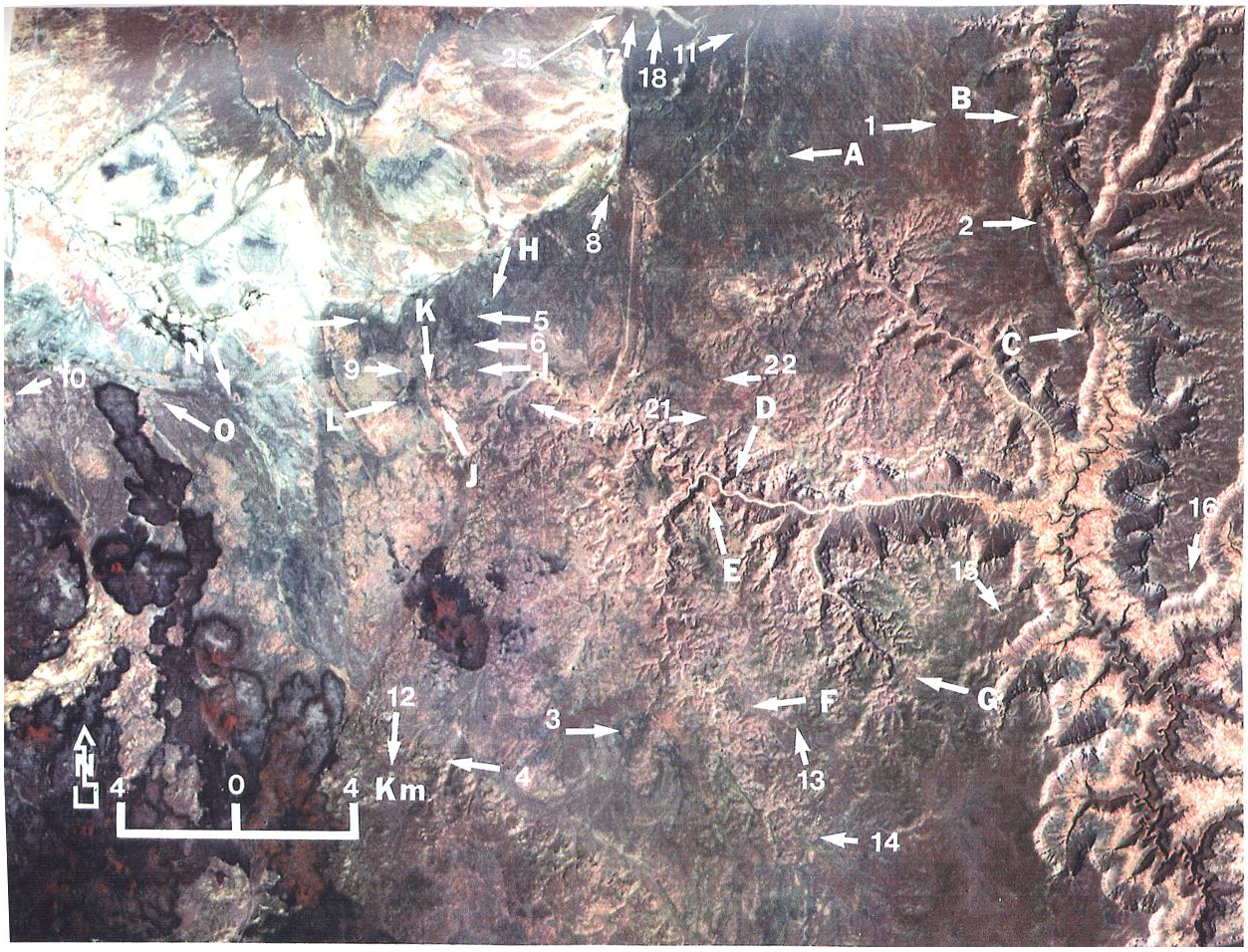
25
7
11
18
B
1
A
2
8
H
K
5
6
N
9
10
O
L
J
22
21
D
C
E
16
15
12
3
F
G
4
13
14
N
4
0
4
Km

Fig. 4.

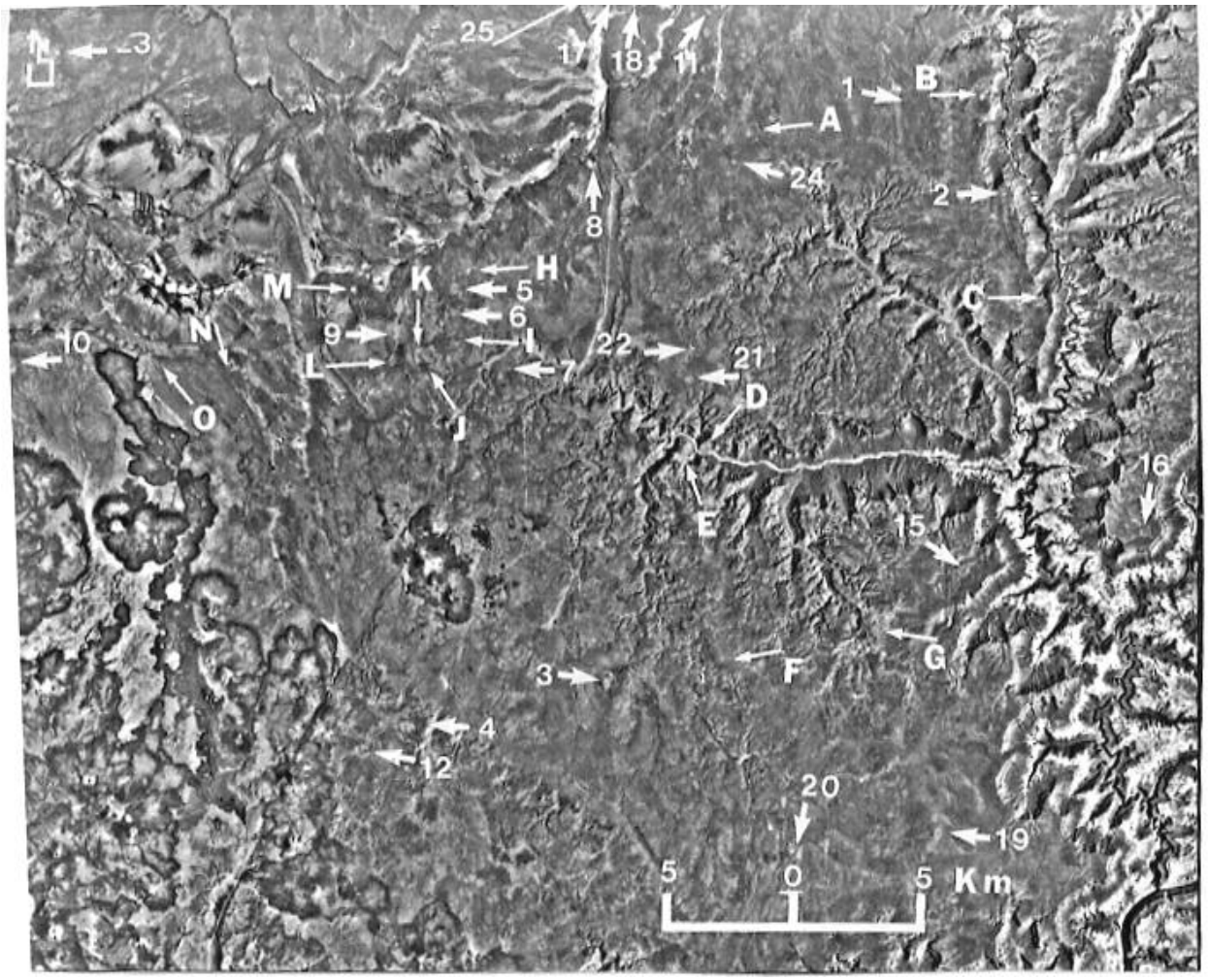
N
3
25
17
18
11
1
B
A
24
2
8
H
M
K
5
6
C
N
9
10
L
22
21
7
D
O
J
16
E
15
G
F
3
4
12
20
19
5
0
5
Km

Fig. 5.

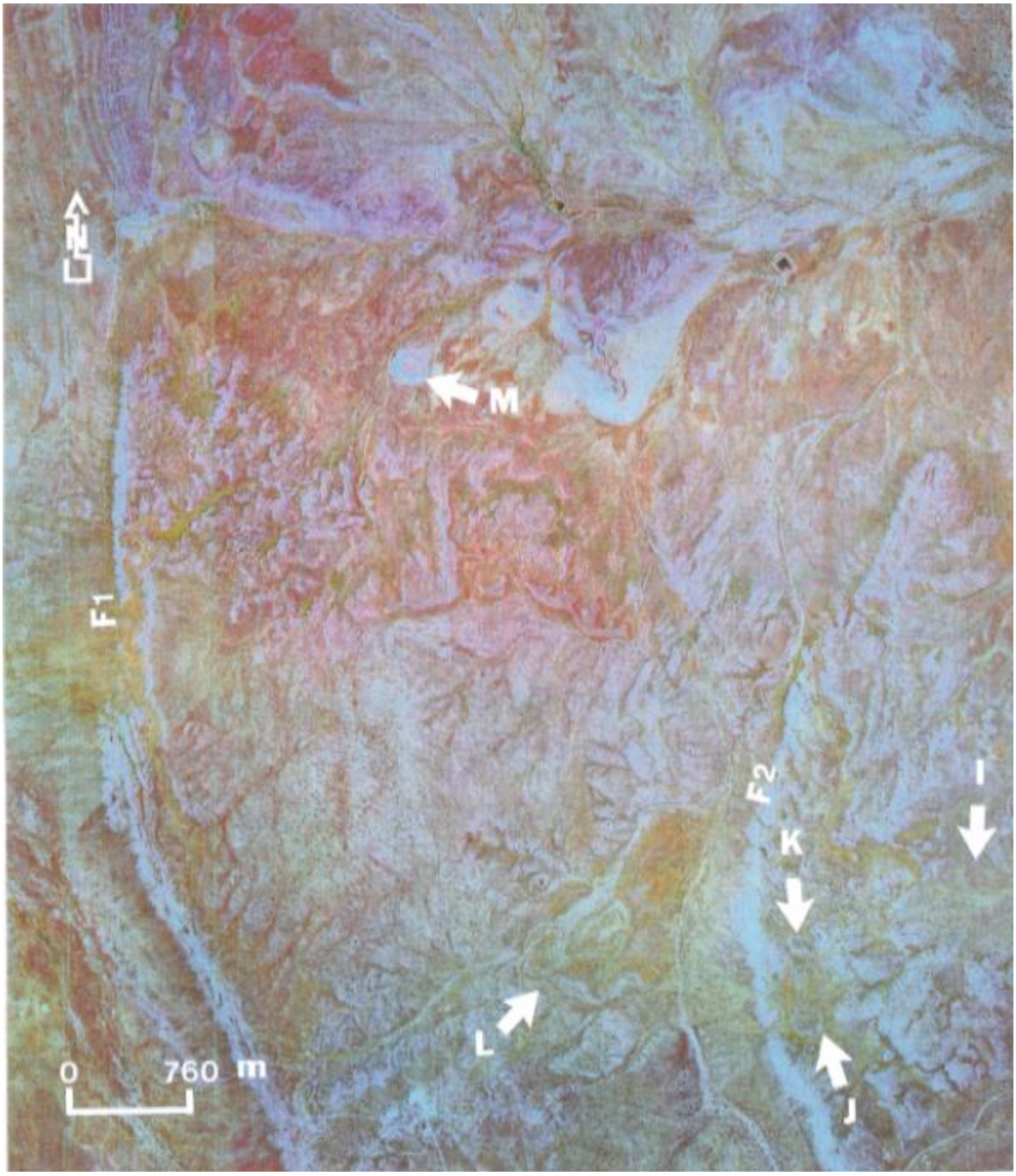

Fig. 6.

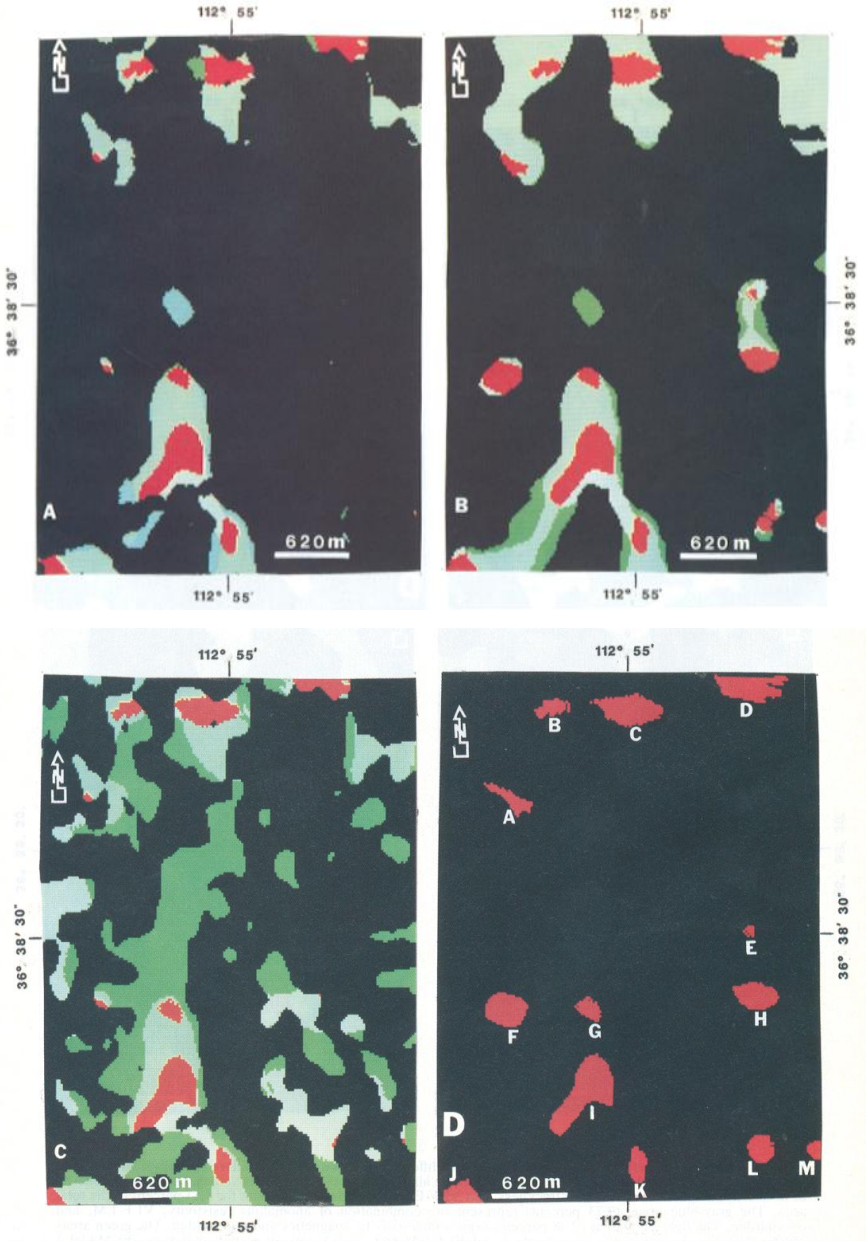

Fig. 7.

Fig. 1. Index map of northwestern Arizona showing the major structural units, the study area, and breccia pipes. Numbers refer to the following breccia pipe names: (1) Grand Gulch, (2) Savannic, (3) Cunningham, (4) Snyder, (5) Old Bonnie Tunnel, (6) Copper House, (7) Copper Mountain, (8) Parashant, (9) Chapel, (10) Ridenour*, (11) Mohawk, (12) Sage, (13) Platinum, (14) Lynx, (15) Rose, (16) SBF, (17) Orphan, (18) Grandview, (19) Canyon, (20) New Year, (21) Black Box, (22) Otto, (23) Riverview, (24) Arizona, (25) Pinenut, (26) Hack 1, (27) Hack 2 &3, (28) Rim, (29) Kanab South, (30) Kanab North, (31) Pigeon, (32) Hermit, (33) DB 1, (34) What, (35) EZ-1, (36) EZ-4 (37) EZ-2, (38) Lisa, (39) John, (40) Peace.
*Old mines (developed before 1980) from which uranium was mined.

Fig. 2. Schematic cross section of a mineralized breccia pipe found in northwestern Arizona (modified after Krewedl and Carisey, 1986

Fig.3. Exposed breccia pipe on the north wall of the Little Colorado River gorge. (A) The surface expression of the pipe, the collapse cone, showing gently dipping beds towards the center of the circular depression. (B) The throat of the pipe which has been partly eroded by the Little Colorado River.

Fig. 4. Landsat TM bands 5, 4 and 3 color composite image of the Hack area. Numeric characters refer to possible potential targets for the occurrence of mineralized breccia pipes. Alphabetic characters refer to the following known breccia pipe deposits or occurrences: (A) Hermit, (B) Kanab North, (C) Rim, (D) Hack 1, (E) Hack 2 and 3, (F) Arizona 1, (G) Pinenut, (H) DB 1, (I) What, (J) EZ-1, (K) EZ-4, (L) EZ-2, (M) Peace, (N) John, and (O) Lisa.

Fig. 5. High-pass filtered (kernel size 51 by 51) Landsat TM band 7 image of the Hack area. Annotations are the same as in Fig. 4.

Fig. 6. Color composite of PC3 (red) PC2 (green) and PC1 (blue) of the digitized blue, green and red components of NHAP photograph of part of the Hack study area. Annotation refers to the know breccia pipes; M Peace, I What, K EZ-1, L EZ-2. F1 and F2 refer to normal faults in the area.

Fig 7. Image results generated from the modeling using different combinations of the filtered geophysical datasets. The red areas (anomalies) correspond to locations where all data sets have anomalously values. (A) Model 1 consists of resistivity, magnetics, overburden thickness, and VLF-EM. The anomalies account for 5.13% of the total area. The gray-blue areas (9.73%) represent the combination of anomalous resistivity, VLF-EM, and overburden. The light-blue areas (2.83%) represent resistivity, magnetics and overburden. The green areas consist of resistivity, magnetics and overburden, and VLF-EM and are 0.8%of the total area (B) Model 2 consists of resistivity, magnetics, and overburden thickness. The red anomalies account for 11.25% of the area. The gray-blue areas (29.04%) represents resistivity and overburden, and the green areas (2.33%) represent magnetics, and overburden. (C) Model 3 consists of resistivity, magnetics, and VLF-EM. The read areas account for 5.68% of the total survey area, the gray-blue areas (magnetics and VLF-EM) 9.0%, and the green (resistivity and VLF-EM) 11.49%. (D) Model 4 consists of resistivity and magnetics. The anomalous areas account for approximately 12.04% of the total area.